# LQG CONTROLLER DESIGNS FROM REDUCED ORDER MODELS FOR A LAUNCH VEHICLE

**Ashwin Dhabale** [*] **Ravi N. Banavar** [**]
**M. V. Dhekane** [***]

[*] *was Graduate student*
[**] *Professor, Systems and Control Engineering*
*IIT Bombay*
[***] *Senior Scientist, ISRO - Thiruvananthapuram, INDIA.*

Abstract: The suppression of liquid fuel slosh motion is critical in a launch vehicle (LV). In particular, during certain stages of the launch, the dynamics of the fuel interacts adversely with the rigid body dynamics of the LV and the feedback controller must attentuate these effects. This paper describes the effort of a multivariable control approach applied to the Geosynchronous Satellite Launch Vehicle (GSLV) of the Indian Space Research Organization (ISRO) during a certain stage of its launch. The fuel slosh dynamics are modelled using a pendulum model analogy. We describe two design methodologies using the linear-quadratic Gaussian (LQG) technique. The novelty of the technique is that we apply the LQG design for models that are reduced in order through inspection alone. This is possible from a perspective that the LV could be viewed as many small systems attached to a main body and the interactions of some of these smaller systems could be neglected at the controller design stage provided sufficient robustness is ensured by the controller. The first LQG design is carried out without the actuator dynamics incorporated at the design stage and for the second design we neglect the slosh dynamics as well. 

Keywords: Launch vehicle, fuel slosh, LQG

## 1. INTRODUCTION

The wave motion of liquids in finite containers, commonly known as slosh, is known to have adverse effects on aerospace vehicles. To mitigate these effects a variety of techniques have been proposed including the use of baffles and dampers. These techniques are inherently passive in nature since energy dissipation is primary goal. To go beyond passive slosh suppression, several researchers have investigated the feasibility of applying active feedback control.

In this paper, the control of a LV with significant fuel slosh dynamics is considered. The objective is to simultaneously control the rigid body motion while suppressing the sloshing of the fuel, using only the control effectors (strap-ons) that act on the rigid vehicle. Suppression of the unactuated fuel slosh degree of freedom must be achieved through the system coupling.

The paper is organized as follows. In section 2 the model of the LV with the actuator and fuel slosh dynamics which has been developed by Vikram Sarabhai Space Center (VSSC) in the form of linear differential equations (perturbation

model) is presented. In section 3 we develop a state space model of the system from the set of descriptor equations. The next section of the paper applies LQG controller synthesis technique to control the LV in the presence of sloshing forces. Simulation results that demonstrate the closed-loop performance are then presented.

## 2. MODEL FORMULATION

The LV dynamic model used is provided by VSSC. The equations derived are similar to those presented for a LV in (Greensite 1972). This model describes linear perturbation dynamics for the pitch plane and includes lateral motion, pitching, rolling, first sloshing mode and second order actuator dynamics. The schematic of the LV is shown in figure 1. Four strap-ons are symmetrically attached on the periphery of the central core. The control input is the nozzle deflection angle. Strap-ons 2 and 4 control the pitching of the LV and all four are responsible for rolling. The variables of interest are the attitude angle

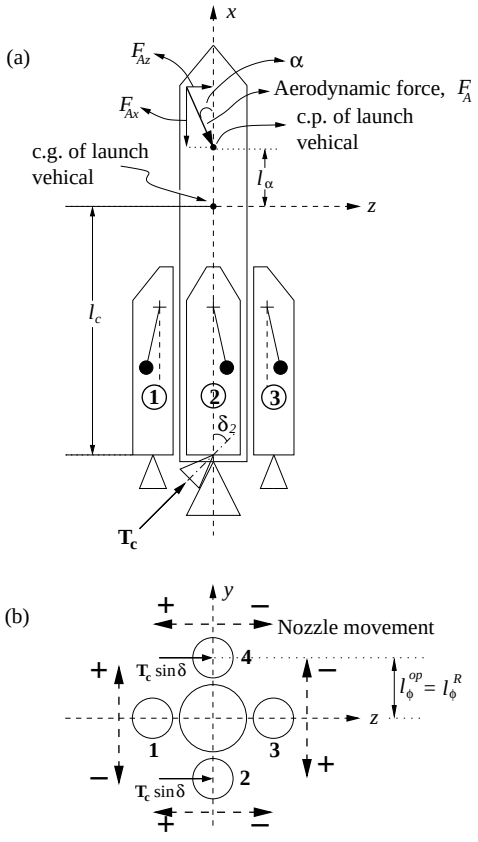


Fig. 1. (a): Schematic of the rocket front view, (b): Schematic of the rocket top view

$\theta$ of the vehicle with respect to a fixed inertial reference, the rolling angle $\phi$ of the vehicle, the actuator deflection angles $\delta_i$ and slosh pendulum angles $\tau_{pi}$ with respect to vehicle longitudinal axis. The mass and moment of inertia of the vehicle and engine are constant in the problem. We now briefly describe the subcomponent dynamics.

### *2.1 Subcomponent dynamics*

Here all the forces and moments are calculated in the pitch $(x - z)$ plane. The component of forces along the vehicle longitudinal axis only accelerate the vehicle and hence are not of interest for control.

*Thrust* Refer to figure 1(a),

$$F_{zT} = T_c \sin\delta_2 \approx T_c\delta_2, \qquad \sin\delta_2 \text{ is small}$$
$$M_{yT} = l_c T_c \delta_2. \tag{1}$$

These expressions are the same for all the nozzles.

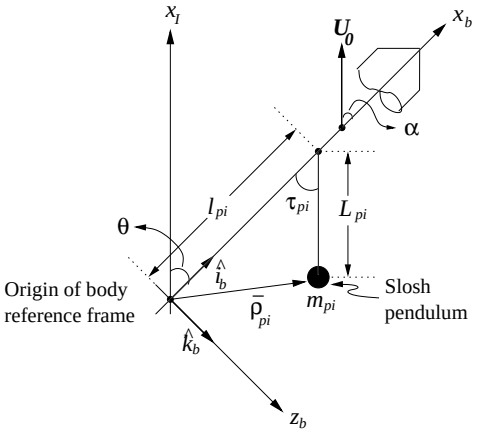


Fig. 2. Schematic of a slosh pendulum

*Sloshing* Consider the schematic of the slosh pendulum shown in figure 2. Using Lagrange's method the sloshing forces and moments can be formulated as

$$F_{zs} = \sum_i m_{pi}\dot{U}_0\tau_{pi}$$
$$M_{ys} = \sum_i m_{pi} l_{pi}\dot{U}_0\tau_{pi}. \tag{2}$$

*Engine inertia* The engine and the launch vehicle are treated as two pendulums connected to each other in the free space, as shown in figure 3. The force exerted by the engine on the vehicle is

$$F_{zE} = m_R l_R \ddot{\delta}_i. \tag{3}$$

The total torque applied to the vehicle in the positive $\theta$ direction due to engine inertia forces is

$$M_{yE} = (I_R + m_R l_R l_c)\ddot{\delta}_i + m_R l_R \dot{U}_0 \delta_i. \tag{4}$$

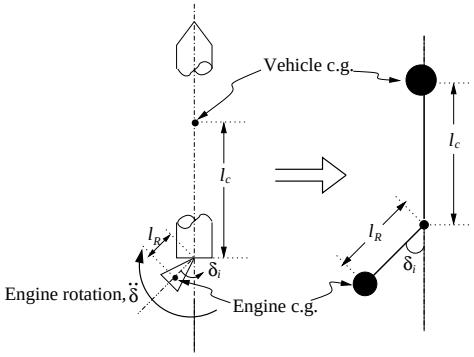


Fig. 3. Engine parameters for single strap-on

*Aerodynamic forces* The aerodynamic force acts at the center of pressure of the LV. It acts along the line of the vehicle velocity as shown in figure 1(a) and can be given as and

$$F_{Az} = L_\alpha \alpha \tag{5}$$

where, $L_\alpha$ is constant of proportionality and depends on vehicle shape, body cross-section area, air density and velocity (Heitchue 1968).

### *2.2 Short period dynamics equations for pitch/roll coupled system*

The forces and moments given in the previous subsection are now incorporated to give the final linearized short period model frozen at an instant and valid for short time. So we have the following equations

*Pitching* All the moments acting about vehicle body $y-$axis are summed to yield

$$I_{yy}\ddot{\theta} = \sum_{i=2,4}(I_R + m_R l_R l_c)\ddot{\delta}_i - \sum_{i=1}^{8}[\dot{U}_0 m_{pi} l_{pi}]\tau_{pi} + [L_\alpha l_\alpha]\alpha + \sum_{i=2,4}(T_c l_c + m_R l_R \dot{U}_0)\delta_i \tag{6}$$

Each strap-on has two compartments one for fuel and the other for oxidizer hence there are total of eight pendulums.

*Lateral motion* All the forces producing the acceleration in the vehicle body $z-$direction are summarized to give

$$(m_0 U_0)(\dot{\alpha} - \dot{\theta}) = \sum_{i=2,4}[m_R l_R]\ddot{\delta}_i + \sum_{i=1}^{8}[m_{pi}\dot{U}_0]\tau_{pi} - [L_\alpha]\alpha + \sum_{i=2,4}[T_c]\delta_i. \tag{7}$$

*Rolling* All the moments in the roll direction give

$$I_{xx}\ddot{\phi} = \sum_{i=1}^{3}[T_c l_{\phi i}^R + m_R \dot{U}_0 l_{\phi i}^R]\delta_i + \sum_{i=1}^{3}[m_R l_R l_{\phi i}^R]\ddot{\delta}_i - [T_c l_{\phi 4}^R + m_R \dot{U}_0 l_{\phi 4}^R]\delta_4 - [m_R l_R l_{\phi 4}^R]\ddot{\delta}_4 + \sum_{1=1}^{8}[m_{pi}\dot{U}_0 l_{\phi i}^{op}]\tau_i. \tag{8}$$

*Slosh* Slosh pendulums have second order dynamics given by

$$\ddot{\tau}_{pi} + 2\zeta_{pi}\omega_{pi}\dot{\tau}_{pi} + \omega_{pi}^2\tau_{pi} = [(l_{pi} - L_{pi})/L_{pi}]\ddot{\theta} - [U_0/L_{pi}]\dot{\alpha} - [l_{\phi i}/L_{pi}]\ddot{\phi} + [U_0/L_{pi}]\dot{\theta} \tag{9}$$

where the terms on the right hand side are forcing functions on the pendulums.

*Actuator dynamics* As shown in figure 3, the nozzle is considered as a pendulum and is modeled as

$$\ddot{\delta}_i = \omega_a^2\delta_c - 2\zeta_a\omega_a\dot{\delta}_i - \omega_a^2\delta_i \tag{10}$$

where $\omega_a$ is the natural frequency, $\zeta_a$ the damping coefficient and $\omega_a^2\delta_c$ is the forcing function, where $\delta_c$ is the desired nozzle deflection. The autopilot command $\delta_P$ for the pitch loop and $\delta_R$ for roll are transformed into four actuator commands as given in the transformation matrix $T$ as follows:

$$\underbrace{\begin{bmatrix}\delta_{1c}\\ \delta_{2c}\\ \delta_{3c}\\ \delta_{4c}\end{bmatrix}}_{\mathbf{u}} = \underbrace{\begin{bmatrix}0 & 1\\ 1 & 1\\ 0 & 1\\ 1 & -1\end{bmatrix}}_{\mathbf{T}} * \underbrace{\begin{bmatrix}\delta_P\\ \delta_R\end{bmatrix}}_{\mathbf{u'}} \tag{11}$$

*Sensors* The sensors are rate and angle gyros modeled as second order systems.

## 3. FORMULATION OF THE STATE SPACE MODEL

The vehicle dynamics including rigid body, slosh and actuators can be written in a descriptor state space form as

$$K\dot{x} = Ax + Bu$$
$$y = Cx + Du \tag{12}$$

where,

$x \in I\!R^{29}$ : the vehicle state vector,
$u \in I\!R^4$ : pitch and roll control signal, defined in (11),
$y \in I\!R^4$ : output vector, $y = [\theta,\ \dot{\theta},\ \phi,\ \dot{\phi}]^T$,

and $A, K, B, C, D$ have appropriate dimensions.

The 29 state variables are $\theta,\ \dot{\theta},\ \alpha,\ \phi,\ \dot{\phi},\ \tau_i,\ \dot{\tau}_i \ldots i = 1$ to 8 and, $\delta_j,\ \dot{\delta}_j \ldots j = 1$ to 4. Rewrite (12) as

$$\dot{x} = A_1 x + B_1 u, \tag{13}$$

where $A_1 = K^{-1}A$ and $B_1 = K^{-1}B$, for $K^{-1}$ exists. The system (13) is a 4 input and 4 output system. The inputs to the system are the desired actuator deflections but the signal generated by the controller are the pitch and roll angles. Hence substituting (11) in (13) gives a 2 input 4 output system,

$$\dot{x} = A_1 x + B_1' u', \tag{14}$$

where, $B_1' = B_1\mathbf{T}$. The system (14) is analyzed and found to be unstable, uncontrollable and unobservable. This makes the system unsuitable for LQG controller design. To circumvent these problems, we carry out some conditioning and model order reduction on the system.

Standard model order reduction techniques are not applicable here due to the unstable nature of the system. The model order is reduced by inspecting the system equations. We return to the system in the form given by (12) for this purpose. It is observed that with some assumptions on the magnitudes of the coefficients in the $K$ matrix, we are able to separate the actuator dynamics as follows.

$$\underbrace{\left[\begin{array}{c|c} K_{11} & K_{12} \\ \hline K_{21} & K_{22} \end{array}\right]}_{K_{29\times 29}} \left[\begin{array}{c} \dot{x}_0 \\ \hline \dot{\Delta} \end{array}\right] = \underbrace{\left[\begin{array}{c|c} A_{11} & A_{12} \\ \hline A_{21} & A_{22} \end{array}\right]}_{A_{29\times 29}} \left[\begin{array}{c} x_0 \\ \hline \Delta \end{array}\right] + \left[\begin{array}{c} B_{11} \\ \hline B_{21} \end{array}\right] u$$

$$\overbrace{\begin{array}{l} \dot{\Delta} = A_{22}\Delta + B_{21}u \\ y_{act} = C_{act}\Delta \end{array}}^{Actuator} \quad \Big\| \quad \overbrace{\begin{array}{l} K_{11}\dot{x}_0 = A_{11}x_0 + B^* y_{act} \\ y = C_0 x_0 \end{array}}^{Rocket}$$

where, $K_{11} \in I\!R^{21\times 21}$ , $K_{12} \in I\!R^{21\times 8}$ and is approximated to zero, $K_{21} = [\mathbf{0}]_{8\times 21}$ and $K_{22} = [\mathbf{I}]_8$. Also $A_{21} = [\mathbf{0}]_{8\times 21}$. $B_{11} \in I\!R^{21\times 4}$ and $B_{21} \in I\!R^{8\times 4}$.

The left hand side set of equations describe an $8^{th}-$order actuator system

$$\begin{aligned} \dot{\Delta} &= A_{act}\Delta + B_{act}u' \\ y_{act} &= C_{act}\Delta \end{aligned} \tag{15}$$

where $\Delta = [\delta_1,\ \dot{\delta}_1, \ldots, \delta_4,\ \dot{\delta}_4]^T, A_{act} = A_{22}, B_{act} = B_{21}\mathbf{T}$ and $y_{act} = [\delta_1,\ \delta_2,\ \delta_3,\ \delta_4]$ is the output of the actuator.The set of equations on the right hand side describes a $21^{st}-$ order rigid body plus slosh system where the terms in $B^*$ are terms in $A_{12}$ corresponding to $\delta_1,\ \delta_2,\ \delta_3$ and $\delta_4$. We rewrite this system as

$$\begin{aligned} K_0\dot{x_0} &= A_0 x_0 + B_0 y_{act} \\ y &= C_0 x_0 \end{aligned} \tag{16}$$

where $x_0$ is a state vector consisting of the 5 rigid body and 16 slosh state variables. Since $K_0$ is invertible we have

$$\begin{aligned} \dot{x_0} &= A_{01}x_0 + B_{01}y_{act} \\ y &= C_0 x_0 \end{aligned} \tag{17}$$

where $A_{01} = K_0^{-1}A_0$ and $B_{01} = K_0^{-1}B_0$. The system (17) is a 4 input and 4 output system. For the purpose of controller design we neglect the actuator dynamics and hence (11), (15) and (17) give a 2 input 4 output system given by

$$\dot{x}_0 = A_{01}x_0 + B_{01}'u' \qquad y = C_0 x_0 \tag{18}$$

where $B_{01}' = B_{01}\mathbf{T}$. The system (18) is controllable and observable though unstable.

## 4. LQG CONTROLLER SYNTHESIS

The expression for the LQG compensator, a dynamic output feedback compensator made up of regulator and filter, is given by

$$\mathbf{u}(s) = -K_c(sI - A + BK_c + K_f C)^{-1}K_f\mathbf{y}(s)$$

where $K_c$ is regulator gain matrix and $K_f$ is Kalman filter gain matrix. The $K_C$ is calculated such that it minimizes the performance criterion

$$J(\mathbf{x}, t_0, T, \mathbf{u}(\cdot)) = \int_{t_0}^{T} [\mathbf{x}^T Q\mathbf{x} + \mathbf{u}^T R\mathbf{u}]dt,$$

and $K_f$ is such that it gives best estimate for the given random process noise and observation noise covariances, $W$ and $V$ respectively. These conditions lead to the Riccatti equations, solving which the gain matrices are obtained (Siouris 1996). The choice of the weighting matrices $Q,\ R,\ W,$ and $V$ is somewhat arbitrary. In this work, all such computations were performed on MATLAB.

### *4.1 Design 1*

Initially the weighting matrices are selected as unity matrices of appropriate size multiplied by a scalar, and by varying the value of the scalar some iterations are done. To obtain a better controller it is essential to vary individual entries in the weighting matrices. Since working with a $21^{st}-$order weighting matrices is difficult, smaller weighting matrices are designed for a $5^{th}-$order rigid body system by neglecting the slosh dynamics. The smaller weightings are selected such that the closed loop with the rigid body dynamics alone exhibits a good response. Then these smaller weighting matrices are inserted into the larger

unity matrices of appropriate size. The weighting matrices hence obtained are

$$\mathbf{Q} = \left[\begin{array}{ccc|c} 100 & 8 & 2 & \\ 8 & 1 & 0.5 & \emptyset \\ 2 & 0.5 & 1 & \\ \hline & \emptyset & & [\mathbf{I}]_{18} \end{array}\right], \quad \mathbf{W} = 4.5[\mathbf{I}]_{21}$$

$$\mathbf{R} = [\mathbf{I}]_2, \qquad \mathbf{V} = [\mathbf{I}]_4.$$

The controller thus obtained has all the poles in left hand $s-$plane, farthest from $Im-$axis is at -90.1860 and nearest is at -0.0003. It places the closed loop poles between $\text{Re}\{p_i\} = -86.1156$ and $\text{Re}\{p_i\} = -0.0211$.

### *4.2 Design 2*

Design 1 gives a $21^{st}-$order controller which may be difficult to implement and will increase the closed-loop order significantly. Hence a controller of smaller order is designed. For this purpose the $5^{th}-$order rigid body system is used.

For selecting the weighting matrices, the rigid body system is further divided into pitch and roll systems. Since the system is a 2 input 4 output one, out of two singular value plots one belongs to the pitch and the other to the roll. The objective is to keep these singular value plots for the closed loop system as close to each other in the bandwidth of operation/interest. The smaller order weighting matrices are then augmented to get a $5^{th}-$order weighting matrix which is further manipulated to get a better performance. The weighting matrices thus obtained are

$$\mathbf{Q} = \text{diag}\ \{20,\ 0.01,\ 0.1,\ 1,\ 1\}, \qquad \mathbf{R} = 10[\mathbf{I}]_2,$$
$$\mathbf{W} = \text{diag}\ \{100,\ 500,\ 0.1,\ 150,\ 150\},$$
$$\mathbf{V} = \text{diag}\ \{10,\ 10,\ 1,\ 1\}.$$

The controller poles are at -3.4018, -0.0252, -8.8524, -15.5837, -12.8088 and the closed-loop poles are located between $\text{Re}\{p_i\} = -76.9718$ and $\text{Re}\{p_i\} = -0.0208$.

## 5. SIMULATION RESULTS

In this section we demonstrate the effectiveness of the controller by performing simulations of the closed-loop shown in figure 4. The closed-loop system is the system between the points 1 and 2, and the output signals plotted are taken from point 3. A step input is applied separately in the pitch and roll channel. The step response, actuator deflection and deflection of the slosh pendulums are plotted. The step is 1° in magnitude and applied at time $t = 0$ sec.

The step response with controller 1 is better for the pitch channel, while the response of the roll

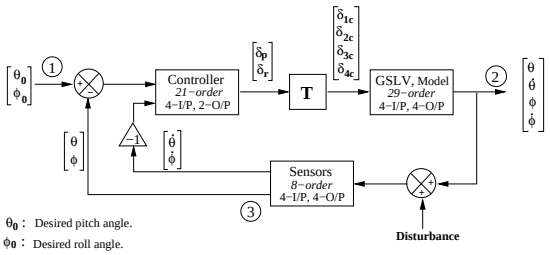


Fig. 4. Closed-Loop block diagram.

channel is better with controller 2 (figure 5). In all the cases the actuator deflections are well within the allowable limits of ±6°, see figure 6. Figure 7 shows sloshing excited due to the application of the step input in the pitch channel. The slosh is suppressed well with controller 1, but in the case of controller 2, the oscillations are sustained for a long period of time indicative of the fact that at the design stage the slosh dynamics was neglected. Figure 8 shows the Nyquist plots for the pitch and

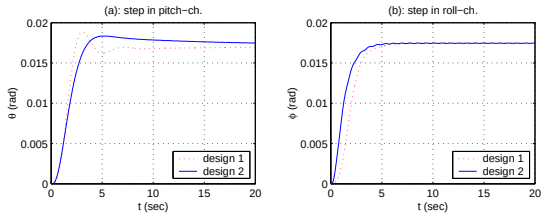


Fig. 5. Closed-loop step response.

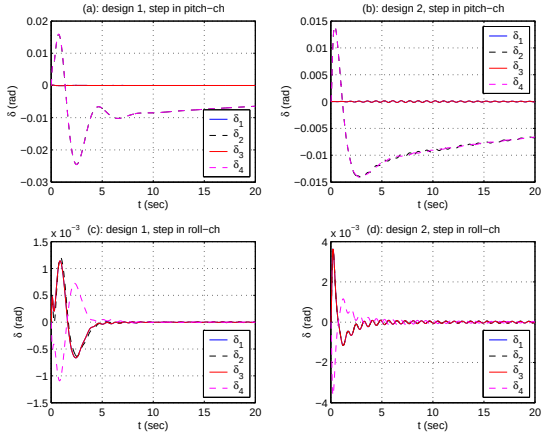


Fig. 6. Actuator deflection corresponding to response plotted in figure 5.

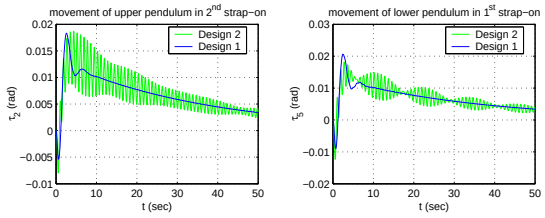


Fig. 7. Fuel slosh in response to step in pitch channel.

roll channel. The pitch channel transfer function (TF) is the TF from $\delta_p$ to $\theta$ and for roll channel it

is the TF from $\delta_r$ to $\phi$. The plot depicts that the gain and phase margins are larger for the system with controller 2. The Bode plots for the same system are shown in figure 9. The phase plot shows the effect of the actuator dynamics on the system phase near 25 rad/sec.

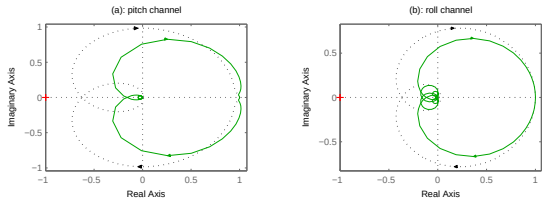


Fig. 8. Nyquist plots, $(\cdots)$ design 1 and $(\text{—})$ design 2.

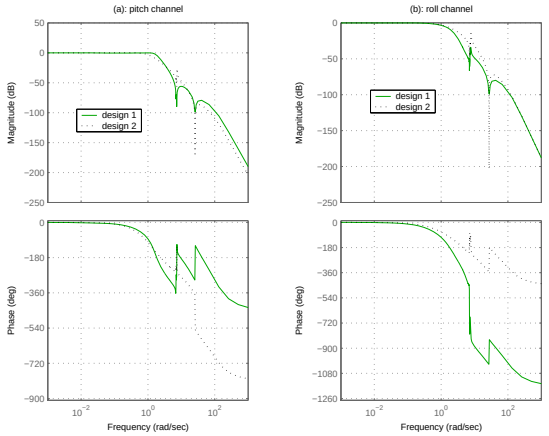


Fig. 9. Bode plot.

## 6. CONCLUSION

In this paper we have synthesized a LQG controller for a $29^{th}-$order perturbation model of a LV. The proper system for LQG design is obtained from the given system by separating the actuator dynamics. If a large system comprises of a main system and many smaller systems coupled to it, then with some assumptions the smaller systems can be decoupled. If a controller is designed for the main system with significant robustness then the original large system can be successfully controlled with the same controller. Here we have presented two such controllers.

## 7. ACKNOWLEDGEMENTS

The authors thank the Indian Space Research Organization (ISRO) for supporting this project through the ISRO-IITB Cell.

## REFERENCES

Greensite, A.L. (1972). *Control Theory: Analysis and Design of Space Vehicle Flight Control Systems.*. Spartan Books.

Heitchue, R. D. Jr. ed. (1968). *Space System Technology*. Reinhold. New York.

Siouris, George M. (1996). *An Engineering Approach to Optimal Control and Estimation Theory*. Jhon Wiley & Sons, Inc.